



Room temperature H₂S gas sensor based on rather aligned ZnO nanorods with flower-like structures



Z.S. Hosseini^a, A. Irajizad^{b,c,*}, A. Mortezaali^a

^a Department of Physics, Alzahra University, Tehran 1993893973, Iran

^b Department of Physics, Sharif University of Technology, Tehran 113659161, Iran

^c Institute for Nanoscience and Nanotechnology, Sharif University of Technology, Tehran 111558639, Iran

ARTICLE INFO

Article history:

Received 9 May 2014

Received in revised form 19 October 2014

Accepted 20 October 2014

Available online 4 November 2014

Keywords:

ZnO

Vapor phase transport

Gas sensor

H₂S

ABSTRACT

Rather vertically aligned ZnO rods with flower-like structures were grown on quartz substrates through vapor phase transport method. X-ray diffraction (XRD) analysis and photoluminescence (PL) measurement were performed to determine crystalline structure and defects, respectively. H₂S gas sensing properties of the grown structure were investigated at both room temperature and 250 °C for comparison. A remarkable increase in response and selectivity at room temperature compared to 250 °C was observed. High response and selectivity to low concentrations of H₂S at room temperature as well as good stability make the sensor a promising candidate for practical applications.

© 2014 Elsevier B.V. All rights reserved.

1. Introduction

Hydrogen sulfide is a poisonous, corrosive and flammable gas which is usually found in crude petroleum, coal, oil and natural gas industries. Its short term (10 min) and long term (8 h) threshold limits are 15 and 10 ppm, respectively. Thus, real time detection in the concentration range (<15 ppm) is the most important for the human health safety [1,2].

Zinc oxide (ZnO) has been widely investigated as a gas sensing material due to its wide range of conductance variability for different structures, good thermal and chemical stability, high electron mobility, and non-toxicity [3–7]. In the recent years, gas sensors based on one-dimensional ZnO nanostructures have attracted much attention due to their advantageous features, such as high sensitivity and low power consumption [4,5]. It is known that a desirable gas sensor should have a combination of high sensitivity and selectivity, long-term stability, low operating temperature, and resistance. These parameters are mainly dependent on effective surface area, defect density, additives, and crystal structure of the sensing layer [6–8]. Different structures of ZnO such as tetrapods and bundle of nanorods have been used previously for fabricating H₂S gas sensors [1,9]. However, these sensors work at temperatures above 250 °C. This results in high power consumption and

restriction for detecting flammable and explosive gases like H₂S with auto ignition 260 °C in normal atmosphere [6,10,11]. Zhang et al. fabricated a H₂S gas sensor based on dendritic ZnO nanorods which operates at room temperature (RT) [6]. Nonetheless, the stability of the reported H₂S sensor is a challenging issue which needs more investigations.

Thick film sensors based on ZnO nanorods were reported by Wang et al. which showed good response to low concentrations of H₂S at room temperature (1.7 to 0.05 ppm) [12]. They coated a paste composed of ZnO nanorods and PVA solution onto an Al₂O₃ tube. However, the fabricated sensor did not reach a steady state even after 25 min of exposure and recovery was not complete after gas removal [13]. Furthermore, electronic integration of thick film gas sensors with other electronic components of the device is difficult [14].

Using single ZnO nanowire has been proposed for detecting flammable gases like H₂ at room temperature [15]. Manipulation and creation of electric contacts with individual nanowire is a complex and tedious process [16]. Datta et al. fabricated room temperature H₂S gas sensors based on the grown random network of ZnO nanowires via hydrothermal method. They improved poor operation of the sensors by modifying the sensing layer with Au [2].

We expect that aligned nanorods provide larger surface area, so we considered this structure for detecting H₂S. There are few studies reporting the improvement in sensing of LPG and H₂ gases by vertically aligned ZnO rods at temperatures above 200 °C [5,17]. To the best of our knowledge, there are no reports on their H₂S

* Corresponding author. Tel.: +98 21 66164513; fax: +98 21 66022711.

E-mail address: iraji@sharif.edu (A.I. Irajizad).

sensing properties at room temperature. Among rather expensive techniques for preparation of the aligned ZnO nanorods such as metal organic vapor phase epitaxy [18] and atomic layer deposition (ALD) [19], chemical processes including chemical bath deposition (CBD) [5], hydrothermal [17,20], and electrochemical [21] methods are cost effective, but they commonly produce structures with low crystallinity and uncontrollable levels of impurities [1,22]. Carbothermal reduction vapor phase transport (CTR-VPT) is a simple method which produces high quality ZnO nanostructures [22]. Since deposition temperature in this method is usually above 600 °C, the grown structures have better thermal and temporal stability.

We synthesized rather vertically aligned rods accompanied by flower-like structures with considerable density of oxygen vacancy through making proper growth conditions via CTR-VPT method. The H₂S gas sensing properties of the grown structure were measured at two operating temperatures, room temperature (RT) and 250 °C. The prepared samples showed higher response to low concentrations of H₂S at room temperature than those reported in the published articles.

2. Experimental

The synthesis process was promoted in a horizontal tube furnace at normal atmosphere pressure. Quartz substrates were put down at definite distance (16.5–17.2 cm) away from the furnace center where a mixture of ZnO and graphite powders (a weight ratio 1:1) as the source material was placed. The source material was heated to 1060 °C at a rate of 20 °C/min and was maintained constant at this temperature for 1 h under 100 sccm constant flow rate of Ar. After the growth, the furnace was cooled down to room temperature naturally.

Tescan (MIRA II LMU MI0430976IR) scanning electron microscope (SEM) was used for investigating the morphology of the

grown structures. Crystalline structure was studied by obtaining X-ray diffraction (XRD) patterns with Cu K α 1 radiation (Panalytical X'Pert Pro MPD, $\lambda = 1.54056 \text{ \AA}$). Photoluminescence (PL) measurement was performed at room temperature by Cary Eclipse-Fluorescence spectrophotometer with a Xe lamp ($\lambda = 325 \text{ nm}$) as the excitation source.

For gas sensing measurements, two gold electrodes (2 mm width, spaced at 1 mm) were thermally evaporated on the ZnO layer. The samples were placed on the holder equipped with a heater and thermocouple. For gas sensing tests, a static-type gas measurement setup consisting of a chamber with 7 L volume, fan, moving arm for placing the holder in the chamber suddenly, feed through for gas injection, and electronic equipment was used. The required concentrations of the target gas were provided by injecting a definite amount of the desired gas. The base gas is ambient air with 25% relative humidity (RH). Target gases are dry and become diluted with ambient air, as the base gas, when injected to the sensing chamber.

Electrical measurements were performed by applying a fixed bias of 5 V across the electrodes and recording the sample current as a function of time by using a Sanwa multimeter interfaced with a computer. The gas response was defined as $S = I_g/I_a$, where I_g and I_a are the current of the sensor in presence of the target gas and air, respectively. The response and recovery times are defined as the required times for 90% of total change in resistance upon exposure to gas and air, respectively.

3. Results and discussion

3.1. Morphology and crystalline structure

Rather vertically aligned nanorods with flower-like structures were observed in SEM images (Fig. 1). Diameter of the rods is in the range of 300–500 nm, and their length is in the range of 7–9.5 μm .

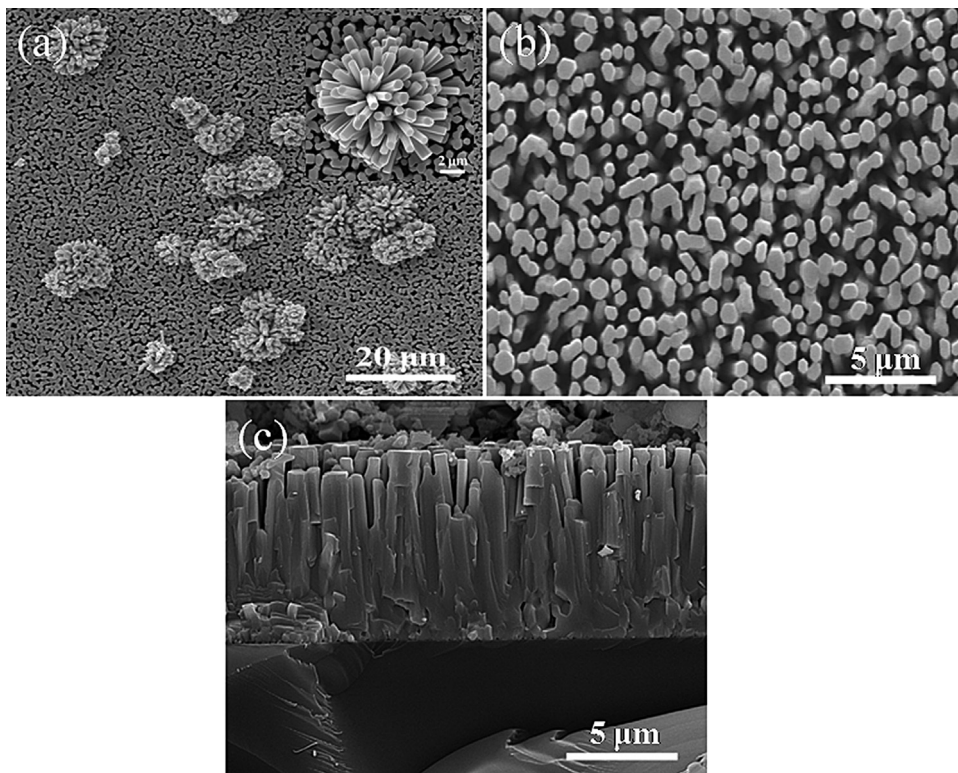


Fig. 1. (a, b) Typical top view and (c) cross section SEM images of the vertically aligned ZnO rods with flower-like structures. Inset of Fig. 1(a) shows magnified image of one of the flowers.

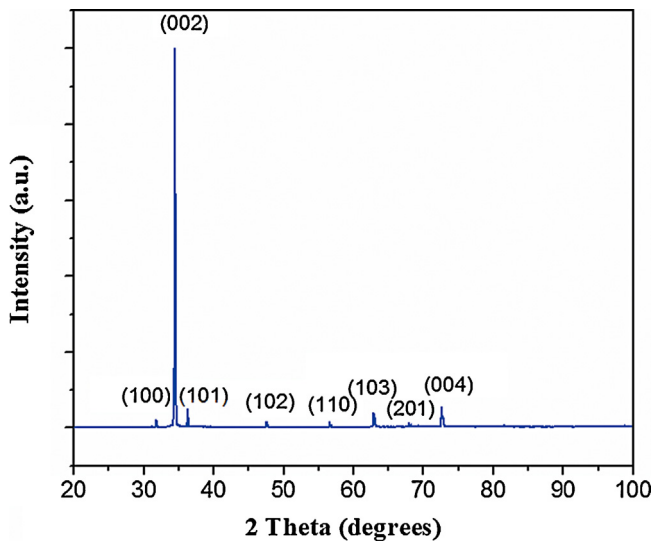


Fig. 2. X-ray diffraction pattern of the prepared ZnO rods.

In this configuration, nanorods form a porous network consisting of directional channels for gas diffusion in and out. The presence of flower-like bundle of rods increases the effective surface area which leads to enhancing gas sensitivity [7]. Concerning the ZnO growth on the whole substrate surface, a continuous electrical path is provided by interconnected nanorods for carrier transport between the two gold electrodes. Details of growth mechanism and structure have been reported elsewhere [23].

Crystallinity of the sensing layer is an effective parameter in the gas sensor operation. Crystalline structure of the grown samples was investigated by performing XRD experiments as shown in Fig. 2. All the peaks in the XRD patterns were well indexed to hexagonal-wurtzite ZnO phase consistent with the standard values in JCPDS card no. 005-0664. The intense (002) peak confirms preferred growth along the *c*-axis. As a result, the most (002) planes are perpendicularly oriented with the substrate surface.

Native defects in ZnO such as oxygen vacancy and zinc interstitial affect the surface chemistry and electronic properties of the sensing material including adsorption reactivity, catalytic activity, and electrical conductivity [24,25]. These parameters are in strong correlation with sensor's operation. PL is a technique for studying defects and their relative density ($I_{\text{def}}/I_{\text{UV}}$ where I_{def} for the defect emission intensity and I_{UV} for the UV emission intensity). Fig. 3 indicates typical room temperature PL spectrum of the as-grown samples. The UV peak is assigned to near band edge (NBE) emission [26]. A narrow peak positioned at 442 nm is attributed to zinc interstitials [27]. Origin of the broad green emission peak is usually referred to irradiative recombination of a photo generated hole with an electron in a singly ionized oxygen vacancy [28,29]. The stronger green emission relative to UV emission is indicating of considerable oxygen vacancy defects in the grown structure. The calculated value of $I_{\text{def}}/I_{\text{UV}}$ is about 2 for the grown structure. A large quantity of oxygen vacancy enhances sensor response through high adsorptions of oxygen which increase the probability of interaction with target gas molecules [24,25,30].

3.2. Gas sensing properties

Fig. 4 shows the sensor response at different temperatures. The response is the highest at room temperature (26 °C) and decreases with increasing temperature. The observed reduction in the sensor response could be related to decreasing sample resistance in air which is originated from the following reasons: (1) oxygen

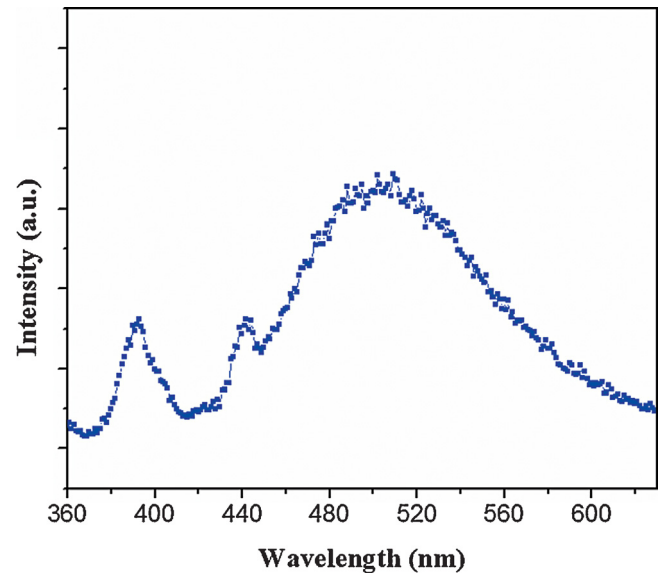


Fig. 3. Room temperature photoluminescence spectrum of the grown ZnO nano-structure.

vacancies in ZnO form intragap states below the conduction band edge so that many of them are shallow donors. Ionization of these states even at room temperature makes the ZnO an n-type semiconductor. By increasing temperature, more intragap states ionize, and density of charge carriers increases [31]. (2) Rising temperature causes enhancement in phonon assisted tunneling which results in reducing resistance [31]. Since the grown structure in this work contains rather high density of oxygen vacancies, distinct change in sensor resistance with elevating temperature seems reasonable.

We compared sensing properties of the fabricated sensors at 250 °C and room temperature (26 °C). As displayed in Fig. 5(a), response as a function of gas concentration exhibit increasing trend with larger values at room temperature. The measured values reveal that the fabricated sensors can detect H₂S in the ppb level. The reported concentration range is of great importance for application in health and safety monitoring [1,2]. At this concentration level the sensors indicate high sensitivity (i.e. the slope of response curve versus concentration) with average value 86 ppm⁻¹. Figs. 5(b) and (c) show the transient response curves of the sensor to 1 and 5 ppm H₂S at RT and 250 °C, respectively. The sensor response

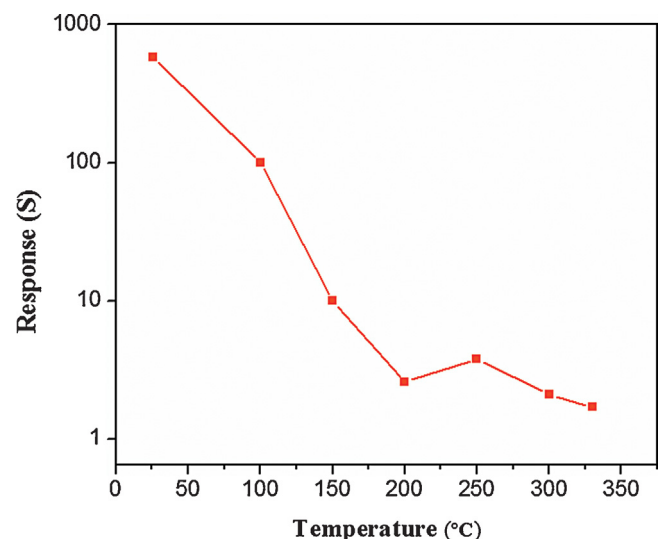


Fig. 4. Sensor response toward 5 ppm H₂S gas at various temperatures.

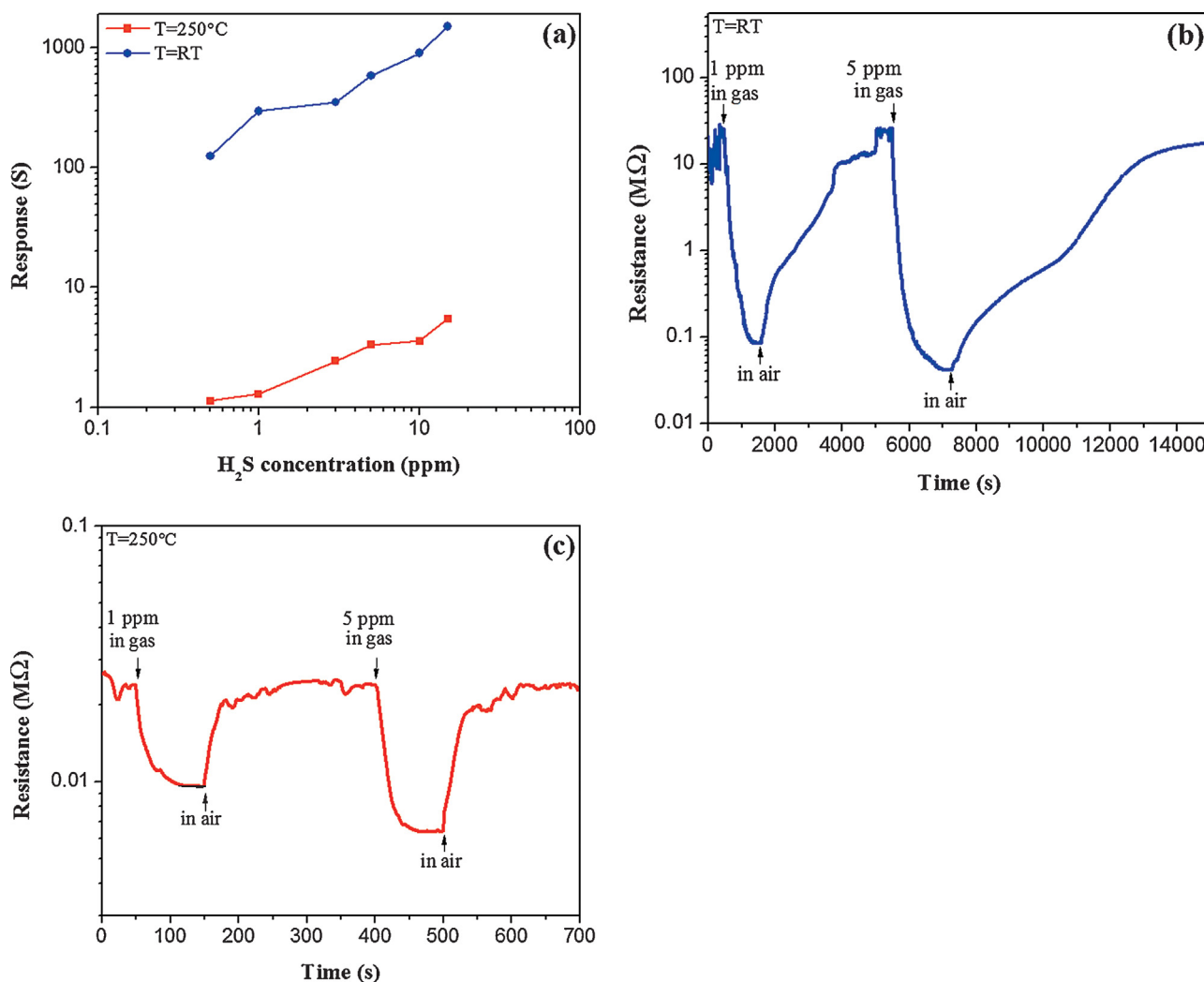
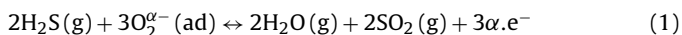


Fig. 5. (a) Sensor response versus different concentrations of air diluted H₂S gas. Time dependence of the sensor resistance upon exposure to 1 and 5 ppm H₂S at (b) room temperature and (c) 250 °C.

toward 1 and 5 ppm of H₂S was found about 296 and 581 at room temperature and 2.4 and 3.7 at 250 °C, respectively. The results showed that both response and recovery times decrease at 250 °C, e.g., response and recovery times for 1 ppm H₂S are 320 and 3592s at RT as well as 27 and 77 s at 250 °C, respectively.

To discuss sensing behavior of our samples, it is known that the response (the change in the resistance) of a resistive metal oxide gas sensor arises from reactions between adsorbed oxygen species and target gas molecules [31]. In air, oxygen molecules adsorb on the ZnO surface by capturing electrons from the conduction band. Upon exposure to H₂S, hydrogen sulfide molecules react with the adsorbed oxygen ions and release the trapped electrons back to the conduction band through the following reaction [9]:



α is 1 or 2 for description of singly or doubly ionized oxygen. Dominant oxygen species are molecular ions (O_2^- , O_2^{2-}) at low temperatures and atomic ions (O^- , O^{2-}) at higher temperatures ($T > 175^\circ\text{C}$) [9,32]. This process increases electron concentration in the rods and decreases band bending which leads to reduction in sensor resistance. The reaction (1) is exothermic, so the molecular water, which is one of the reaction products, desorbs quickly from the surface. Humidity influences sensing performances of oxide semiconductors especially at room temperature [6,33]. The

measured sensor response to humidity at RT was found to be 1.5, 2.5 and 2.9 after exposure to ~66%, ~75% and ~90% relative humidity, respectively which are several ten times lower than response to H₂S. During measurements, the RH levels were being monitored constantly by a standard hygrometer. Proton hopping and the Grotthuss chain reaction, capillary condensation, and displacement of adsorbed oxygen species by water molecules have been known as the humidity detection mechanisms [34–36]. More studies are in progress for describing the humidity sensing mechanism of the grown structure. For considering the influence of humidity on the sensor response to H₂S, at first the sensor resistance became stable at desired RH and then, H₂S gas was introduced. It is observed from Fig. 6 that sensor response decreases to very small amounts with increasing humidity level to values above ~50% which could be described by the following aspects. H₂O molecules are in competition with oxygen for occupying the surface sites. With increasing humidity, more H₂O molecules adsorb so that density of the adsorbed oxygen is reduced leading to a decrease in the sensor response [33,37,38]. Furthermore, decreasing the baseline resistance of the sensor in humid atmosphere could have a contribution in lowering the response [38].

Rather high performance of our samples compared to those reported in literature (see Table 1) can be explained by the following aspects: (a) considerable concentration of oxygen vacancies, (b)

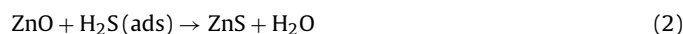
Table 1Reported H₂S gas sensors based on various ZnO nanostructures.

Sensing element	Gas con. (ppm)	Operating temperature (°C)	Response	Response def. (S =)	Ref.
ZnO dendrites	100	30	17.3	R_a/R_g	[6]
ZnO nanorods	5	RT	65	R_a/R_g	[12]
ZnO nanowires network	5	RT	5	I_g/I_a	[2]
Pillar shaped ZnO nanorods	100	50	61.7	$\Delta G/G_{air}$	[39]
ZnO thin film	20	300	22%	$(R_a - R_g)/R_a \times 100$	[3]
Hierarchically porous ZnO	50	332	200	R_a/R_g	[40]
ZnO nanorod-bundle	50	500	35	$(I_g - I_a)/I_a$	[9]
ZnO tetrapods	5	300	100	$\Delta G/G_{air}$	[1]
α -Fe ₂ O ₃ nanochains	5	285	4.7	R_a/R_g	[41]
Fe ₂ O ₃ loaded NiO nanoplates	10	200	7.35	R_a/R_g	[42]
Porous α -Fe ₂ O ₃ nanospheres	10	350	12.9	R_a/R_g	[43]
Aligned ZnO nanorods with flower-like structures	5	RT	581	I_g/I_a	This work

relatively large effective surface area of the grown structure, and (c) good connection between the rods and the presence of interface layer. Although the interface layer can provide direct path for moving electrons, contribution of contact barriers between the rods in the electron transport could not be ignored completely. Upon exposure to H₂S gas, the width and height of the barriers reduce as a result of oxygen coverage reduction. By increasing temperature, charge carriers attain energy to traverse the barriers. Thereby, variation of the barriers by H₂S gas does not have considerable effect on the sensor resistance. This could lead to the reduction in the sensor response at 250 °C.

Furthermore, temperature influences adsorption and desorption rates (of oxygen, reducing gas and reaction products), surface decomposition rate of the reducing gases, charge carrier concentration, and Debye length [44]. Considering the size of the rods, changes of Debye length with temperature do not affect the sensor resistance [45]. By rising temperature to 250 °C, desorption probability of O₂ and gas molecules enhances. Also, a large fraction of oxygen vacancy defects are activated so that electron concentration and consequently electrical conductance increase. Enhancement of electron concentration obscures the effects of the gas to be detected and lowers the gas sensitivity [46,47]. In other words, increase in electroconductivity reduces the influence of surface reactions on the density of electrons leading to drastic reduction of the response at 250 °C. In addition, rates of H₂S decomposition and sorption processes as well as chemical reaction accelerate at 250 °C which result in decreasing response and recovery times.

Selectivity and stability of the sensing device are very important for practical application. The response to various gases at RT and 250 °C has been depicted in Fig. 7. It shows a good selectivity to H₂S especially at RT. Good selectivity of the sensors can be attributed to high reactivity of H₂S and smaller bond energy of H-SH compared with the other tested gas molecules (as shown in Table 2). H₂S can be decomposed at lower temperature to participate in reaction with sensing material [2,12,40]. Although the bond energy of acetone is close to H₂S, interaction strength between the sensing layer and target gas is an effective factor on the sensor response [5,14,40]. ZnO has higher affinity to H₂S as a strong reducing gas compared to other tested gases [40]. This is explained with adsorption of H₂S by ZnO surface and its decomposition to HS and then to S through the following reaction [50]:



This reaction is an exothermic and spontaneous process [9] which has been known the reason for higher response of ZnO to H₂S [40,50]. However, the reactions between ZnO and other test gases are endothermic and cannot be spontaneous [40]. The required energy for reaction (2) could not be supplied at temperatures below 200 °C [1], therefore the surface reaction of H₂S with adsorbed oxygen species (see reaction (1)) has been considered as the dominant sensing mechanism at $T < 300$ °C [2,6,9,12] which has been demonstrated through XPS analysis by Kim et al. [9].

Temporal and thermal stability of the sensor have been investigated by repeating experiments for 5 ppm H₂S at 250 °C. Fig. 8 displays the measured values for sensor response versus the storing time in normal air atmosphere. Good sensing behavior was

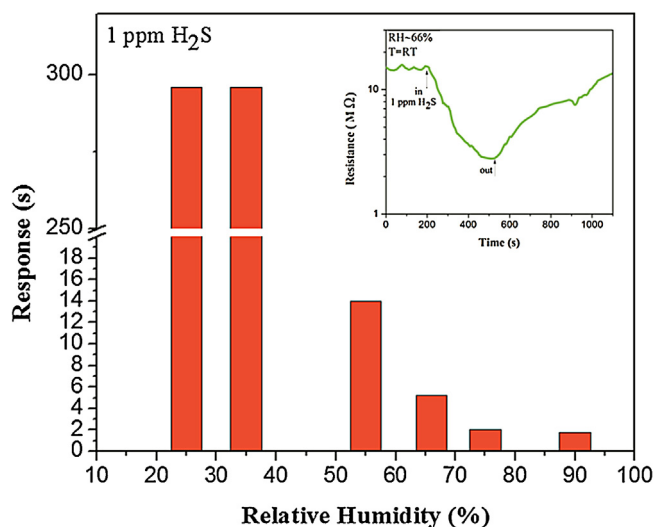


Fig. 6. Sensor response to 1 ppm H₂S gas in the presence of different relative humidities at room temperature. The inset shows typical transient resistance response of the sensor toward 1 ppm H₂S at ~66% RH.

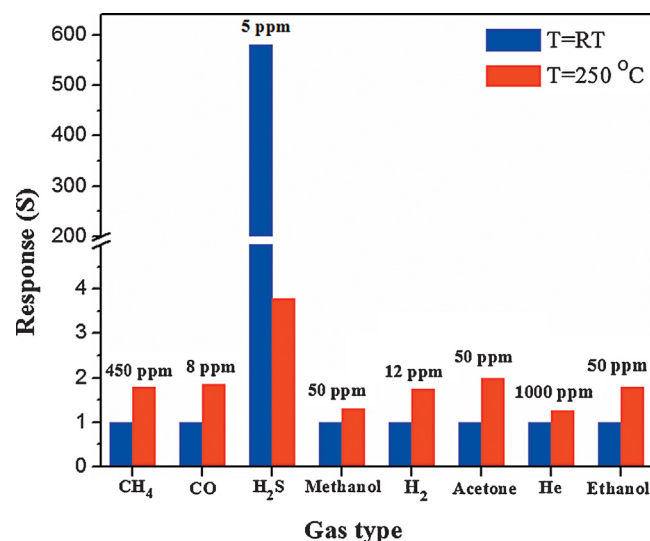


Fig. 7. Sensor response to different reducing gases at room temperature and 250 °C.

Table 2
Properties of the tested gas molecules [48,49].

Gas name	H ₂	CO	Acetone	Ethanol	Methanol	CH ₄	H ₂ S
Structural formula	H—H	C—O	$\begin{array}{c} \text{H} & \text{O} & \text{H} \\ & & \\ \text{H}-\text{C}-\text{C}-\text{C}-\text{H} \\ & & \\ \text{H} & & \text{H} \end{array}$	$\begin{array}{c} \text{H} & \text{H} \\ & \\ \text{H}-\text{C}-\text{C}-\text{O}-\text{H} \\ & \\ \text{H} & \text{H} \end{array}$	$\begin{array}{c} \text{H} \\ \\ \text{H}-\text{C}-\text{O}-\text{H} \\ \\ \text{H} \end{array}$	$\begin{array}{c} \text{H} \\ \\ \text{H}-\text{C}-\text{H} \\ \\ \text{H} \end{array}$	$\text{H}-\text{S}-\text{H}$
Bond	H—H	C—O	H—CH ₂ COCH ₃	H—OC ₂ H ₅ H—CH ₂ H—CH	H—OCH ₃ H—CH ₂ H—CH	H—CH ₃	H—HS
Bond energy (kJ/mol)	436.0	1076.5	393	436.0 473 452	436.8 473 452	431	381

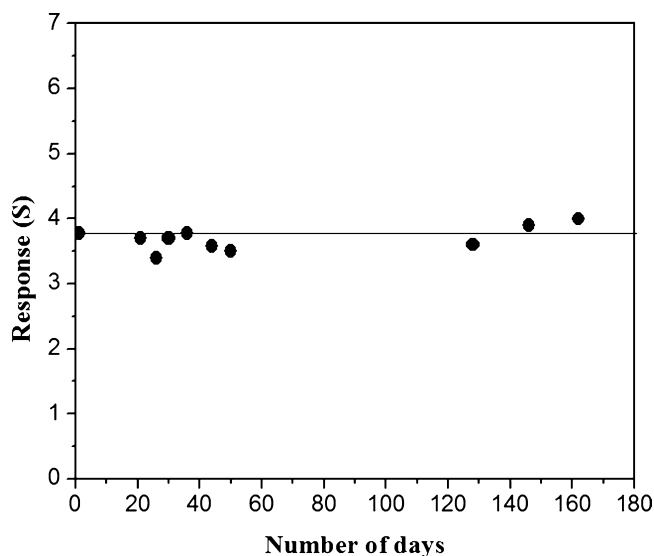


Fig. 8. Variation in the sensor response to 5 ppm H₂S at 250 °C for different periods of time.

observed even after more than 5 months storage in air. High stability indicates stable morphology and good crystallinity of the fabricated sensing layer.

4. Conclusions

Simple vapor phase transport (VPT) method was employed to synthesize relatively ordered array of vertical nanorods accompanied by flower-like structures. The prepared samples exhibited good crystallinity with preferential c-axis orientation and considerable quantity of oxygen vacancy. H₂S sensing properties of the grown structures were tested at room temperature and 250 °C. A high response (e.g. $S=296$ at 1 ppm and 581 at 5 ppm) and good selectivity at room temperature were observed. Response and recovery times decreased with increasing temperature to 250 °C.

Acknowledgement

The authors would like to thank Dr. Roghayeh Ghasempour who helped in some experiments.

References

- [1] D. Calestani, M. Zha, R. Mosca, A. Zappettini, M.C. Carotta, V.D. Natale, L. Zanotti, Growth of ZnO tetrapods for nanostructure-based gas sensors, *Sens. Actuators B* 144 (2010) 472–478.
- [2] N.S. Ramgir, P.K. Sharma, N. Datta, M. Kaur, A.K. Debnath, D.K. Aswal, S.K. Gupta, Room temperature H₂S sensor based on Au modified ZnO nanowires, *Sens. Actuators B* 186 (2013) 718–726.
- [3] P.S. Shewale, B.N. Kamble, A.V. Moholkar, J.H. Kim, M.D. Uplane, Influence of substrate temperature on H₂S gas sensing properties of nanocrystalline zinc oxide thin films prepared by advanced spray pyrolysis, *IEEE Sens. J.* 13 (2013) 1992–1998.
- [4] N. Datta, N. Ramgir, M. Kaur, S.K. Ganapathi, A.K. Debnath, D.K. Aswal, S.K. Gupta, Selective H₂S sensing characteristic of hydrothermally grown ZnO-nanowires network tailored by ultrathin CuO layers, *Sens. Actuators B* 166–167 (2012) 394–401.
- [5] K.V. Gurav, P.R. Deshmukh, C.D. Lokhande, LPG sensing properties of Pd-sensitized vertically aligned ZnO nanorods, *Sens. Actuators B* 151 (2011) 365–369.
- [6] N. Zhang, K. Yu, Q. Li, Z.Q. Zhu, Q. Wan, Room-temperature high sensitivity H₂S gas sensor based on dendritic ZnO nanostructure with macroscale in appearance, *J. Appl. Phys.* 103 (2008) 104305.
- [7] R.C. Pawar, J.S. Shaikh, S.S. Suryavanshi, P.S. Patil, Growth of ZnO nanodisk, nanospindles and nanoflowers for gas sensor: PH dependency, *Curr. Appl. Phys.* 12 (2012) 778–783.
- [8] G. Korotcenkov, The role of morphology and crystallographic structure of metal oxides in response of conductometric-type gas sensors, *Mater. Sci. Eng. R* 61 (2008) 1–39.
- [9] J. Kim, K. Yong, Mechanism study of ZnO nanorod-bundle sensors for H₂S gas sensing, *J. Phys. Chem. C* 115 (2011) 7218–7224.
- [10] J. Gong, Y. Li, X. Chai, Z. Hu, Y. Deng, UV-light-activated ZnO fibers for organic gas sensing at room temperature, *J. Phys. Chem. C* 114 (2010) 1293–1298.
- [11] D.S.J. Jones, Refinery safety measures and handling of hazardous materials, in: D.S.J. Jones, P.R. Pujadó (Eds.), *Handbook of petroleum processing*, Springer, The Netherlands, 2006, pp. 675–705.
- [12] C. Wang, X. Chu, M. Wu, Detection of H₂S down to ppb levels at room temperature using sensors based on ZnO nanorods, *Sens. Actuators B* 113 (2006) 320–323.
- [13] M. Kaur, S. Bhattacharya, M. Roy, S.K. Deshpande, P. Sharma, S.K. Gupta, J.V. Yakhmi, Growth of nanostructures of Zn/ZnO by thermal evaporation and their application for room-temperature sensing of H₂S gas, *Appl. Phys. A* 87 (2007) 91–96.
- [14] Y. Zeng, T. Zhang, M. Yuan, M. Kang, G. Lu, R. Wang, H. Fan, Y. He, H. Yang, Growth and selective acetone detection based on ZnO nanorod arrays, *Sens. Actuators B* 143 (2009) 93–98.
- [15] O. Lupan, G. Chai, L. Chow, Novel hydrogen gas sensor based on single nanorod, *Sens. Actuators B* 85 (2008) 2220–2225.
- [16] G. Korotcenkov, B.K. Cho, The role of grain size on the thermal instability of nanostructured metal oxides used in gas sensor applications and approaches for grain-size stabilization, *Prog. Cryst. Growth Charact. Mater.* 58 (2012) 167–208.
- [17] J.X. Wang, X.W. Sun, Y. Yang, H. Huang, Y.C. Lee, O.K. Tan, L. Vayssieres, Hydrothermally grown oriented ZnO nanorod arrays for gas sensing applications, *Nanotechnology* 17 (2006) 4995–4998.
- [18] W.I. Park, D.H. Kim, S.W. Jung, G.C. Yi, Metalorganic vapor-phase epitaxial growth of vertically well-aligned ZnO nanorods, *Appl. Phys. Lett.* 80 (2002) 4232.
- [19] Y.H. Chang, S.M. Wang, C.M. Liu, C. Chen, Fabrication and characteristics of self-aligned ZnO nanotube and nanorod arrays on Si substrates by atomic layer deposition, *J. Electrochem. Soc.* 157 (2010) K236–K241.
- [20] M. Guo, P. Diao, S. Cai, Hydrothermal growth of well-aligned ZnO nanorod arrays: dependence of morphology and alignment ordering upon preparing conditions, *J. Solid State Chem.* 178 (2005) 1864–1873.
- [21] C. Xu, J.H. Lee, J.C. Lee, B.S. Kim, S.W. Hwang, D. Whang, Electrochemical growth of vertically aligned ZnO nanorod arrays on oxidized bi-layer graphene electrode, *CrystEngComm* 13 (2011) 6036–6039.
- [22] D. Yu, T. Trad, J.T. McLeskey Jr., V. Craciun, C.R. Taylor, ZnO nanowires synthesized by vapor transport deposition on transparent oxide substrates, *Nanoscale Res. Lett.* 5 (2010) 1333–1339.
- [23] Z.S. Hosseini, A. Mortezaali, A. Irajizad, Comparative study of the grown ZnO nanostructures on quartz and alumina substrates by vapor phase transport method without catalyst: synthesis and acetone sensing properties, *Sens. Actuators A* 212 (2014) 80–86.
- [24] Y. Zhang, J. Xu, Q. Xiang, H. Li, Q. Pan, P. Xu, Brush-like hierarchical ZnO nanostructures: synthesis, photoluminescence and gas sensor properties, *J. Phys. Chem. C* 113 (2009) 3430–3435.

- [25] O. Lupan, V.V. Ursaki, G. Chai, L. Chow, G.A. Emelchenko, I.M. Tiginyanu, A.N. Gruzintsev, A.N. Redkin, Selective hydrogen gas nanosensor using individual ZnO nanowire with fast response at room temperature, *Sens. Actuators B* 144 (2010) 56–66.
- [26] Q. Yang, K. Tang, J. Zuo, Y. Qian, Synthesis and luminescent property of single-crystal ZnO nanobelts by a simple low temperature evaporation route, *Appl. Phys. A* 79 (2004) 1847–1851.
- [27] J. Liu, S. Lee, Y.H. Ahn, J.Y. Park, K.H. Koh, Tailoring the visible photoluminescence of mass-produced ZnO nanowires, *J. Phys. D: Appl. Phys.* 42 (2009) 095401.
- [28] Y. Li, G.W. Meng, L.D. Zhang, Ordered semiconductor ZnO nanowire arrays and their photoluminescence properties, *Appl. Phys. Lett.* 76 (2000) 2011–2013.
- [29] Y.J. Xing, Z.H. Xi, Z.Q. Xue, X.D. Zhang, J.H. Song, R.M. Wang, J. Xu, Y. Song, S.L. Zhang, D.P. Yu, Optical properties of the ZnO nanotubes synthesized via vapor phase growth, *Appl. Phys. Lett.* 83 (2003) 1689.
- [30] M.W. Ahn, K.S. Park, J.H. Heo, J.G. Park, D.W. Kim, K.J. Choi, J.H. Lee, S.H. Hong, Gas sensing properties of defect-controlled ZnO-nanowire gas sensor, *Appl. Phys. Lett.* 93 (2008) 263103.
- [31] P. Feng, Q. Wan, T.H. Wang, Contact-controlled sensing properties of flowerlike ZnO nanostructures, *Appl. Phys. Lett.* 87 (2005) 213111.
- [32] R. Nowrouzi, F. Razi, F. Rahimi, A. Irajizad, Catalytic effect of copper oxide on H₂S sensing properties of nanostructured WO₃, *Sens. Lett.* 11 (2013) 1–6.
- [33] G.K. Mani, J.B.B. Rayappan, A highly selective room temperature ammonia sensor using spray deposited zinc oxide thin film, *Sens. Actuators B* 183 (2013) 459–466.
- [34] Y. Shimizu, H. Arai, T. Seiyama, Theoretical studies on the impedance-humidity characteristics of ceramic humidity sensors, *Sens. Actuators B* 7 (1985) 11–22.
- [35] Q. Kuang, C. Lao, Z.L. Wang, Z. Xie, L. Zheng, High-sensitivity humidity sensor based on a single SnO₂ nanowire, *J. Am. Chem. Soc.* 129 (2007) 6070–6071.
- [36] P.K. Kannana, R. Saraswathia, J.B.B. Rayappanb, A highly sensitive humidity sensor based on DC reactive magnetron sputtered zinc oxide thin film, *Sens. Actuators A* 164 (2010) 8–14.
- [37] D. Zappa, E. Comini, G. Sberveglieri, Thermally oxidized zinc oxide nanowires for use as chemical sensors, *Nanotechnology* 24 (2013) 444008.
- [38] S.S. Kim, H.G. Na, S.W. Choi, D.S. Kwak, H.W. Kim, Novel growth of CuO-functionalized, branched SnO₂ nanowires and their application to H₂S sensors, *J. Phys. D: Appl. Phys.* 45 (2012) 205301.
- [39] S.D. Shinde, G.E. Patil, D.D. Kajale, V.B. Gaikwad, G.H. Jain, Synthesis of ZnO nanorods by spray pyrolysis for H₂S gas sensor, *J. Alloys Compd.* 528 (2012) 109–114.
- [40] Z. Liu, T. Fan, D. Zhang, X. Gong, J. Xu, Hierarchically porous ZnO with sensitivity and selectivity to H₂S derived from biotemplates, *Sens. Actuators B* 136 (2009) 499–509.
- [41] J. Ma, L. Mei, Y. Chen, Q. Li, T. Wang, Z. Xu, X. Duan, W. Zheng, α -Fe₂O₃ nanochains: ammonium acetate-based ionothermal synthesis and ultrasensitive sensors for low-ppm-level H₂S gas, *Nanoscale* 5 (2013) 895–898.
- [42] F. Li, Y. Chen, J. Ma, Fe³⁺ facilitating the response of NiO towards H₂S, *RSC Adv.* 4 (2014) 14201–14205.
- [43] J. Deng, J. Ma, L. Mei, Y. Tang, Y. Chen, T. Lv, Z. Xu, T. Wang, Porous α -Fe₂O₃ nanospheres-based H₂S sensor with fast response, high selectivity and enhanced sensitivity, *J. Mater. Chem. A* 1 (2013) 12400–12403.
- [44] A.P. Lee, B.J. Reedy, Temperature modulation in semiconductor gas sensing, *Sens. Actuators B* 60 (1999) 35–42.
- [45] N. Hongsih, E. Wongrat, T. Kerdcharoen, S. Choopun, Sensor response formula for sensor based on ZnO nanostructures, *Sens. Actuators B* 144 (2010) 67–72.
- [46] V. Brinzari, G. Korotcenkov, V. Golovanov, Factors influencing the gas sensing characteristics of tin dioxide films deposited by spray pyrolysis: understanding and possibilities of control, *Thin Solid Films* 391 (2001) 167–175.
- [47] C.S. Prajapati, P.P. Sahay, Influence of In doping on the structural, optical and acetone sensing properties of ZnO nanoparticulate thin films, *Mater. Sci. Semicond. Process.* 16 (2013) 200–210.
- [48] T.W. Swaddle, *Inorganic Chemistry: An Industrial and Environmental Perspective*, Academic Press, USA, 1997.
- [49] D. Zhang, *Morphology Genetic Materials Templated from Nature Species*, Springer, New York, 2012.
- [50] D. Wang, X. Chu, M. Gong, Hydrothermal growth of ZnO nanoscrewdrivers and their gas sensing properties, *Nanotechnology* 18 (2007) 185601.

Biographies

Z.S. Hosseini received the M.Sc. degree in condensed matter physics from Alzahra University, Tehran, Iran, in 2009. She is currently a Ph.D. candidate in physics at Alzahra University. Her research fields include preparation process of nanostructures and their application as gas sensors.

A. Irajizad received her Ph.D. degree in surface physics from Sussex University in 1990. She is a professor in Physics Department at Sharif University of Technology. Her main interest is experimental surface physics, thin films and nanotechnology. She is currently involved in research and development of gas sensors for domestic application.

A. Mortezaali received his Ph.D. from Toulouse University of Paul-Sabatier, France in 1980. The major field in his Ph.D. was Materials and compounds. Currently he is working on condensed matter physics, TiO₂ and ZnO nanostructures, and their applications as a sensor. He has been in an academic position in Department of Physics at Alzahra University, Tehran, Iran since 1990. Currently, he has a Professor Ship in Department of Physics. He is teaching B.Sc., M.Sc., and Ph.D. level students and doing research.